Generating random media from limited microstructural information via stochastic optimization

D. Cule and S. Torquato
Princeton Materials Institute, Princeton University, Princeton, New Jersey 08544

(Received 23 February 1999; accepted for publication 16 June 1999)

Random media abound in nature and in manmade situations. Examples include porous media, biological materials, and composite materials. A stochastic optimization technique that we have recently developed to reconstruct realizations of random media (given limited microstructural information in the form of correlation functions) is investigated further, critically assessed, and refined. The reconstruction method is based on the minimization of the sum of squared differences between the calculated and reference correlation functions. We examine several examples, including one that has appreciable short-range order, and focus more closely on the kinetics of the evolution process. The method is generally successful in reconstructing or constructing random media with target correlation functions, but one must be careful in implementing an earlier proposed time-saving step when treating random media possessing significant short-range order. The issue of the uniqueness of the obtained solutions is also discussed. © *1999 American Institute of Physics.* [S0021-8979(99)06218-0]

I. INTRODUCTION

The generation of realizations of random heterogeneous materials with specified but limited microstructural information is an intriguing inverse problem of both fundamental and practical importance. By limited microstructural information, we mean lower-order statistical correlation functions. A successful means of generating realizations in this way opens up a variety of interesting applications. First, one can identify the class of microstructures that have exactly the same lower-order correlation functions. One can then probe the extent to which the effective properties (e.g., electromagnetic[1,2] elastic moduli,[3–5] and fluid permeability[6–8]) of this class of microstructures vary. Identification of microstructures with the same lower-order correlation functions, but widely different effective properties would be extremely interesting. Second, one can determine the extent to which a variety of different correlation functions can reproduce the reference microstructure, thus shedding light on the nature of the information contained in the correlation functions. Third, one can attempt to reconstruct the full three-dimensional structure of the heterogeneous material from lower-order information extracted from two-dimensional plane cuts through the material.[9] This is of great practical value since in practice one often only has two-dimensional information such as a micrograph or image. Fourth, one can ascertain whether the standard two-point correlation, accessible experimentally via scattering, can reproduce the material. Fifth, one can *construct* structures that correspond to specified correlation functions and categorize random media. Moreover, this exercise can provide guidance in ascertaining the mathematical properties that physically realizable correlation functions must possess. Sixth, one can probe the interesting issue of nonuniqueness given limited microstructural information. Finally, we note that a successful procedure to reconstruct or construct random media can be employed to investigate any physical phenomena where the understanding of spatiotemporal patterns is fundamental, e.g., turbulence.[10]

A popular reconstruction procedure is the one based on the use of Gaussian random fields. The mathematical background used in the statistical topography of Gaussian random fields was originally established in the work of Rice[11] and its survey is given in Ref. 12. Many variations of this method have been developed and applied since then.[13] The Gaussian field approach assumes that the spatial statistics of a two-phase random media can be completely described by specifying only the volume fraction and standard two-point correlation function. This generation is numerical in most cases. The method has been critiqued in Ref. 9. Suffice it to say here that to reproduce Gaussian statistics it is not enough to impose conditions on the first two cumulants only, but also to simultaneously ensure that higher-order cumulants vanish.[14] In addition, the method is not suitable for extension to non-Gaussian statistics, and hence is model dependent.

Recently, we have introduced another stochastic reconstruction technique.[9,15] In this method, one starts with a given, arbitrarily chosen, initial configuration of random medium and a set of reference functions. The medium can be a dispersion of particle-like building blocks[15] or, more generally, a digitized image.[9] The reference functions describe the desirable statistical properties of the target medium, which can be various correlation functions taken either from experiments, theoretical considerations, or just an intuitive ansatz. The method proceeds to find a realization (configuration) in which calculated correlations functions best match the reference functions. This is achieved by minimizing the sum of squared differences between the calculated and reference functions via stochastic optimization techniques, such as the simulated annealing method.

This method is applicable to multidimensional and multiphase media, and is highly flexible to include any type and number of correlation functions as microstructural informa-

tion. It is both a generalization and simplification of the aforementioned Gaussian field reconstruction technique. Moreover, it does not depend on any particular statistics.

In this article, we critically review the details of the method based on minimization of the objective function by simulated annealing technique[9] and discuss the applicability of some other, easy to implement, optimization methods. The limitations and strengths of the studied methods are outlined and addressed via several examples. In particular, we focus our attention on the kinetics of the evolution process and on constructions of structures with appreciable amounts of short-range correlations. We find that the method is able to give reliable microstructures but one must be careful in implementing an earlier proposed time-saving step when treating random media possessing significant short-range order. The uniqueness of the obtained solutions is also discussed. This is an important practical question since the uniqueness is closely related to the reliability of the information extracted from the generated structures. Using a system of randomly distributed overlapping disks, we show that although the obtained solutions are not statistically unique, they remarkably are able to capture salient features of higher-order microstructural information.

The rest of this article is organized as follows. In Sec. II we briefly introduce the basic quantities used in description of random media. In Sec. III the (re)construction procedure is formulated as an optimization problem. In Sec. IV, we study several examples and the details of the simulation kinetics. The previous method is critically assessed and refined. Discussion of other optimization methods and the uniqueness of the generated solutions is given in Sec. V and Sec. VI contains concluding remarks.

II. DESCRIPTION OF RANDOM MEDIA

Consider a digitized image representing a random medium. Different colors (in discrete coloring scheme) describing different phases of the medium may have numerous interpretations. The image can reflect different properties, such as the geometry captured by photographic picture, topology of temperature and scalar velocity fields in fluids, distribution of magnitudes of electric and magnetic fields in the medium, or variations in chemophysical properties of the medium. In the latter case, typical examples are composite materials in which the different phases may have different dielectric, elastic, or absorbing properties, to name a few. To characterize an M-component multiphase system, in which each phase has volume fraction ϕ_i, $i=1,\ldots,M$, it is customary to introduce the indicator function $I^{(i)}(\mathbf{r})$ defined as

$$I^{(i)}(\mathbf{r})=\begin{cases}1, & \text{if } \mathbf{r} \text{ lies in phase } i,\\ 0, & \text{otherwise.}\end{cases} \tag{1}$$

The statistical characterization of the spatial variations of the multiphase systems involves the calculation of n-point correlation functions:

$$S_n^{(i)}(\mathbf{r}_1,\mathbf{r}_2,\cdots,\mathbf{r}_n)=\langle I^{(i)}(\mathbf{r}_1)I^{(i)}(\mathbf{r}_2)\cdots I^{(i)}(\mathbf{r}_n)\rangle. \tag{2}$$

The angular brackets $\langle\cdots\rangle$ denote ensemble averaging over independent realizations of samples. We assume that system is statistically *homogeneous* which implies that ensemble averaging can be replaced by volume averaging. In practice, this ergodic property is often relaxed and required only for the first- and second-order correlations which, in most cases, are the only measured or calculated quantities.

The most basic information on volume composition and interfacial surface area is contained in the lowest-order correlation functions. The average of $I^{(i)}(\mathbf{r})$ is equivalent to the volume fraction of the phase i:

$$\langle I^{(i)}(\mathbf{r})\rangle=\phi_i, \tag{3}$$

and is the probability that the randomly chosen point belongs to phase i. Global information about the surface of the ith phase may be obtained by ensemble averaging the gradient of $I^{(i)}(\mathbf{r})$. Since $\nabla I^{(i)}(\mathbf{r})$ is different from zero only on the interfaces of the ith phase, the corresponding specific surface s_i (defined as the total area of the interfaces divided by the volume of the medium) is given by

$$s_i=\langle|\nabla I^{(i)}(\mathbf{r})|\rangle. \tag{4}$$

The two-point correlation function $S_2^{(i)}(\mathbf{r}_1,\mathbf{r}_2)$ is interpreted as the probability that two randomly chosen points $\mathbf{r}_1$ and $\mathbf{r}_2$ lie in phase i. For statistically isotropic media, rotational symmetry implies $S_2^{(i)}(\mathbf{r}_1,\mathbf{r}_2)=S_2^{(i)}(|\mathbf{r}_1-\mathbf{r}_2|)$.

Much attention has been devoted to studies of properties of the two-point autocorrelation function $S_2^{(i)}(\mathbf{r}_1,\mathbf{r}_2)$ which, for isotropic media, is defined as

$$S_2^{(i)}(r)\equiv\frac{1}{\Omega}\int_\Omega S_2^{(i)}(\mathbf{r})d\Omega, \tag{5}$$

where $\mathbf{r}=\mathbf{r}_1-\mathbf{r}_2$, and the integral over Ω is D-dimensional averaging over all directions of $\mathbf{r}$. In the absence of long-range order, the $S_2^{(i)}(r)$ have the characteristic asymptotic behavior: $S_2^{(i)}(r\to 0)=\phi_i$, and $S_2^{(i)}(r\to\infty)=\phi_i^2$. The autocorrelation functions contain information on the specific surfaces as well. For a two-phase continuum medium, it was shown[16] that the specific surface s_i is proportional to the derivative of $S_2^{(i)}(r)$. In particular, for two-dimensional digitized media, the relation reads: $s_i=-4[dS_2^{(i)}(r)/dr]_{r=0}$. More information on the distribution of surfaces between different phases can be obtained by computing various correlations of $\nabla I^{(i)}(\mathbf{r})$, $i=1,2,\ldots,M$.

The calculation of higher-order correlation functions encounters both analytical and numerical difficulties, and very few experimental results needed for comparison purposes are available so far. However, their importance in the description of collective phenomena is indisputable. A possible pragmatic approach is to study more complex lower-order correlation functions. For instance, the two-point cluster function $C_2^{(i)}(\mathbf{r}_1,\mathbf{r}_2)$ is defined as the probability that two randomly chosen points $\mathbf{r}_1$, and $\mathbf{r}_2$ belong to the same cluster of phase i.[2] Another function characterizing clustering (to a lesser degree) is the ''*lineal-path*'' function $L^{(i)}(\mathbf{r}_1,\mathbf{r}_2)$, defined as the probability that the entire line segment between points $\mathbf{r}_1$ and $\mathbf{r}_2$ lie in phase i. As previously in the limit $|\mathbf{r}_1-\mathbf{r}_2|\to 0$, $L^{(i)}$ gives appropriate volume fraction:

$$L^{(i)}(r)|_{r=0}=\phi_i. \tag{6}$$

III. STOCHASTIC OPTIMIZATION PROCEDURE

For simplicity, we will drop the superscript i to denote the phase of interest. The phase of interest will be stated explicitly. Consider a given set of correlation functions $f_n^\alpha(\mathbf{r}_1,\mathbf{r}_2,\cdots,\mathbf{r}_n)$ that provides partial information on the random medium. The index α is used to denote the type of correlation function. The information contained in the given set of correlation functions could be obtained either from experiments or it could represent a hypothetical medium based on simple models. In both cases we would like to generate the underlying microstructure with a specified set of correlation functions. In the former case, the formulated inverse problem is frequently referred to as a ''reconstruction'' procedure, and in the latter case as a ''construction.''

It is natural to formulate the described (re)construction problem as an optimization problem. The best generated structure is chosen so that the discrepancies between its statistical properties and the imposed ones is minimized. This can be readily achieved by introducing the ''*energy*'' function E defined as a sum of squared differences between target correlation functions, which we denote by $\tilde{f}_n^\alpha$, and those calculated from generated structure, f_n^α.[17] Hence,

$$E=\sum_{\mathbf{r}_1,\mathbf{r}_2,\cdots,\mathbf{r}_n}\sum_{\alpha}\left[f_n^\alpha(\mathbf{r}_1,\mathbf{r}_2,\cdots,\mathbf{r}_n)-\tilde{f}_n^\alpha(\mathbf{r}_1,\mathbf{r}_2,\cdots,\mathbf{r}_n)\right]^2. \tag{7}$$

The optimization technique suitable for the problem at hand is the method of simulated annealing.[18] It has been a favorite method in the optimization of large-scale problems, especially those where a global minimum is hidden among many local extrema. The concept of finding the lowest energy state by simulated annealing is based on a well-known physical fact: If a system is heated to a high temperature T and then slowly cooled down to absolute zero, the system equilibrates to its ground state. At a given temperature T, the probability of being in a state with energy E is given by the Boltzmann distribution $P(E)\sim\exp(-E/T)$. At each annealing step k, the system is allowed to evolve long enough to thermalize at $T(k)$. The temperature is then lowered according to a prescribed annealing schedule $T(k)$ until the energy of the system approaches its ground state value within an acceptable tolerance. It is important to keep the annealing rate slow enough in order to avoid trapping in some metastable states.

In our problem, the discrete configuration space includes the states of all possible elementary block (pixel) allocations. Starting from a given state, a new state can be obtained by interchanging two arbitrarily selected pixels of different phases. This simple sampling procedure preserves the volume fraction of all involved phases and guarantees ergodicity in the sense that each state is accessible from any other state by a finite number of interchange steps.

To evolve the system towards its minimum energy state, we choose the Metropolis algorithm as the acceptance criterion. In this case, the logarithmic annealing schedule which decreases the ''temperature'' according to $T(k)\sim 1/\ln(k)$ would evolve the system to its ground state. A logarithmic decrease may cause very slow convergence. Thus, we will adopt the more popular and faster annealing schedule $T(k)/T(0)=\lambda^k$, where constant λ is the annealing rate which must be less than but close to one.[18] This may yield suboptimal results but, for practical purposes, will be sufficient. The convergence to an optimum is no longer guaranteed, and the system is likely to freeze in one of the local minima if the thermalization and annealing rate are not adequately chosen. Other optimization methods described elsewhere could be employed as well. Some of these will be addressed in Sec. V.

The construction of a system with more complicated correlation functions may require large, time-consuming, optimization procedures. This may be unacceptable in many potential applications. It is therefore preferable to use an evolution scheme (such as Metropolis combined with simulated annealing) which can be continuously monitored, and, if necessary, interrupted as soon as one is satisfied with the obtained resolution. This can enormously shorten the (re)construction time. In many practical applications there is no need for knowing the details of the configurations.[19]

The complexity of the (re)construction is reflected in the kinetics of the simulation process. Thus, in order to understand the abilities and limitations of the advocated procedure, we first investigate the simulation kinetics.

IV. EXAMPLES AND SIMULATION KINETICS

The collective behavior of a many-body system is noticeable in a region within a few correlation lengths. Correlations are a consequence of various interactions present in the system and they are crucial for the understanding of global properties. The (re)construction procedure, which can successfully build-in significant correlations in the system, in a controllable way, is of particular practical interest. Thus, we focus our studies on such systems, focusing on several illustrative two-dimensional examples.

Nontrivial correlation functions are those imposing long-range order. Additional difficulties are possible as well, for example, if correlations do not have rotational symmetry. Since we have formulated the problem in statistical terms, requiring that each sample is statistically homogeneous, the correlation length must be much smaller than the size of the investigated system. There are, however, important exceptions. It is enough to consider translationally invariant systems within their basic cells, mimicking the rest of the structure by periodic boundary conditions. In general, each time periodic boundary conditions are applied, the system is effectively infinitely large and the change of averaging implied in Eq. (2) (from ensemble to volume averaging) is justified. However, the system size must be large enough to ensure that imposed boundary conditions do not affect the original structure. We will exploit this fact in the examples which follow.

As illustrative examples, we investigate both deterministic, crystal-like structures, and random systems that are based on common, analytically studied models. In the case of completely deterministic structures we will show how the reconstruction procedure efficiently leads to the exact solu-

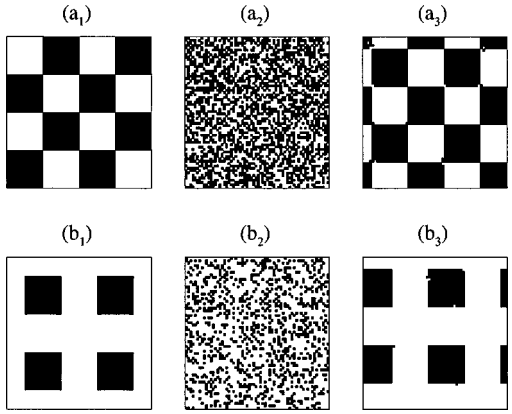

FIG. 1. Reconstruction of regular (a) checkerboard and (b) array of squares with periodic boundary conditions. Figures (a_1), (b_1); (a_2), (b_2); and (a_3), (b_3) show target, initial, and reconstructed configurations, respectively.

tion. However, the optimization of disordered and frustrated structures is significantly harder. To speed up the computational procedure, we will relax the optimization constraints on $S_2(r)$ which is informationally the most important quantity. Results obtained by several optimization techniques will be detailed and discussed.

A. Deterministic structures: Regular array of square-shaped inclusions

First, we consider a specific two-dimensional and two-phase structure composed of a square array of square-shaped inclusions (see Fig. 1). This morphology may be viewed as a cross section of two-phase materials containing rod- or fiber-like inclusions. Various transport properties of these materials have been well explored because of their practical and theoretical importance in materials science and optics.[20]

The special square-array structure is a regular checkerboard with equal volume fractions of white and black phases, i.e., $\phi_1=1/2$ and $\phi_2=1/2$. This is illustrated in Fig. 1(a_1). Another realization of the square array with particular choice $\phi_1=3/4$ and $\phi_2=1/4$ is shown in Fig. 1(b_1). We take these two configurations as our test cases to reconstruct them following the procedure laid out in Sec. III using only the two-point correlation functions of the black phase: $S_2(\mathbf{r})=\langle I(\mathbf{r}_1)I(\mathbf{r}_1-\mathbf{r})\rangle$, and the known volume fractions ϕ_i, $i=1,2$.

Let $\tilde{S}_2(\mathbf{r})$ be the known ''target'' correlation function which can be readily calculated from the original target configuration. Then, according to Eq. (7), the energy function which has to be minimized is $E=\Sigma_{\mathbf{r}}[S_2(\mathbf{r})-\tilde{S}_2(\mathbf{r})]^2$. To employ the simulated annealing minimization technique, we first discretize the system by introducing an $L_x\times L_y$ lattice. The simulations start from random initial configurations [as those shown in Figs. 1(a_2) and 1(b_2)], at some initial temperature T_0, with fixed volume fractions ϕ_i. At each Monte Carlo (MC) step, when an attempt to exchange two randomly chosen pixels of black and white phases is made, $S_2(\mathbf{r})$ is calculated in momentum space using an efficient fast Fourier transform (FFT) algorithm. Using $S_2(\mathbf{r})$, we can calculate the energy between the old and new configurations, and make an appropriate evolution move according to the Metropolis algorithm. At each temperature, the system is thermalized until either $N_{\mathrm{MC}}=\lambda_{\mathrm{MC}}L_xL_y$ MC moves are accepted or the total number of attempts to change the original configurations reaches $N_{\mathrm{tot}}=\lambda_{\mathrm{tot}}L_xL_y$. Subsequently, the system temperature is decreased by the annealing rate λ: $T_{\mathrm{new}}=\lambda T_{\mathrm{old}}$. The choice of the constants λ_{MC}, λ_{tot}, and λ specifies the annealing schedule.

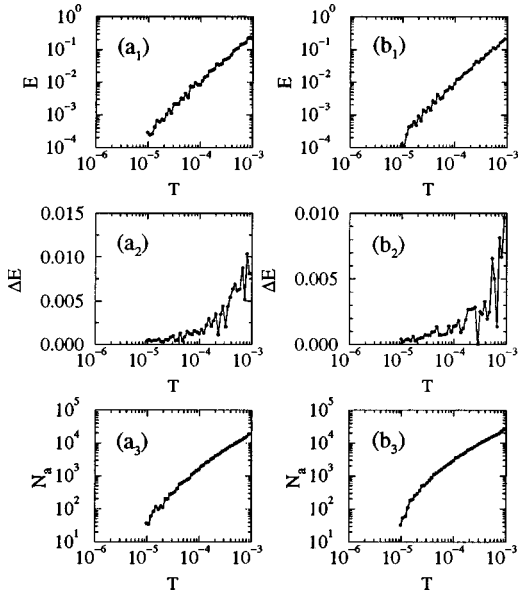

FIG. 2. ''Temperature'' dependence of configuration energy E, change in energy $\Delta E=E_{\mathrm{old}}-E_{\mathrm{new}}$, and number of accepted MC moves N_a for regular (a) checkerboard and (b) array of squares shown in Fig. 1.

The reconstructions shown in Figs. 1–3 were performed with the parameters $L_x=L_y=64$, $T_0=10^{-3}$, $\lambda_{\mathrm{MC}}=10$, $\lambda_{\mathrm{tot}}=100$, and $\lambda=0.9$. Figure 1 depicts the target, initial, and reconstructed configurations. The reconstructions are practically perfect. A very few misallocations could be easily fixed by running the simulations a bit longer. Thus, we are able to reconstruct the original structure using only information on the one- and two-point correlation functions. For these particular cases, the underlying regular deterministic structures are completely defined by their two-point correlation functions $S_2(\mathbf{r})$.

Details of the simulation kinetics are shown in Fig. 2. The configurational energy E, change in energy ΔE between old and new configuration at the last MC attempt at given temperature, and the total number of accepted moves N_a are shown as function of the annealing temperature T. The reconstructed correlation functions $S_2(\mathbf{r})$ are shown in Fig. 3. We notice that the differences between S_2 and $\tilde{S}_2$ are minimized in all directions of $\mathbf{r}$. This is necessary since these systems are not rotationally isotropic. In the following examples, we will relax these constraints.

B. Hypothetical medium with short-range correlations

Fluids (gases and liquids) are systems with a high degree of symmetry as they are spatially homogeneous and rotationally isotropic. This implies that the environment at any point in a fluid is statistically the same as any other point and independent of the direction. Correlations in the fluids are

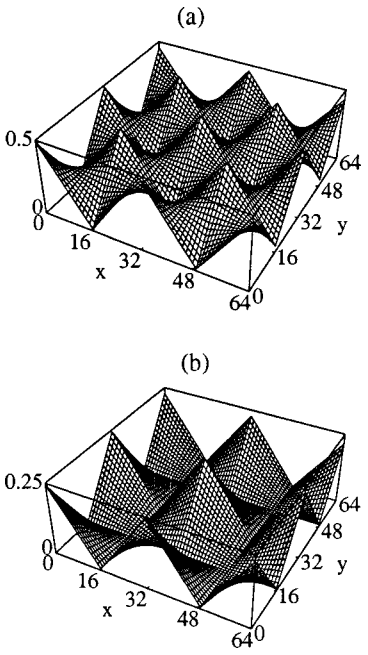

FIG. 3. Reconstructed correlation functions $S_2(\mathbf{r})$ (vertical axis) for reconstruction by FFT of regular (a) checkerboard and (b) array of squares shown in Figs. $1(a_3)$ and $1(b_3)$, respectively.

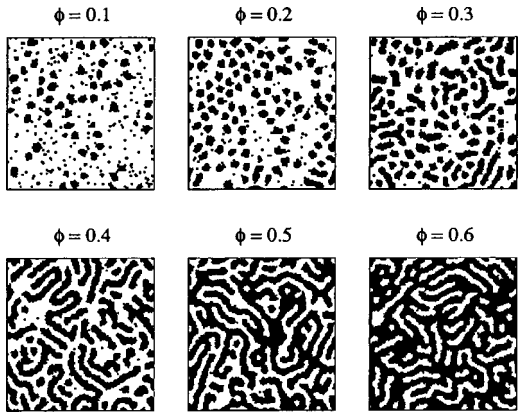

FIG. 4. Structures generated on the basis of target correlation function given by Eq. (8) with $r_0=32$, and $a_0=8$, for various densities ϕ_2 of black phase. Parameters used in simulations are $L_x=L_y=128$, $T_0=5\times10^{-4}$, $\lambda_{\mathrm{MC}}=10$, $\lambda_{\mathrm{tot}}=100$, and $\lambda=0.9$. Periodic boundary conditions are imposed in the x, and y directions, and $S_2(r)$ is calculated from $S_2(\mathbf{r})$ which is obtained using the FFT technique.

primarily due to short-range repulsive interactions. Thus, even the simplest model of fluids, such as a hard-sphere system can capture the basic structure of the fluid.[21] In addition to the temperature driven gas–liquid phase transition in which there is no symmetry change, there can be a liquid–solid transition that is mainly determined by repulsive interactions and hence depends upon density as well. With the increase of liquid density, depending on interparticle interactions, the system may rearrange itself in a regular, equilibrium crystalline solid.

As an example of a statistical construction, we will now generate a two-dimensional and two-phase hypothetical random medium based only on several assumptions. First we assume homogeneity and rotational isotropy to hold independently of the system density. This is a reasonable assumption for low-density fluids and amorphous solids which do not have long-range order. Examples of amorphous materials include porous media, randomly polymerized plastics, and glasses. A glass may alternatively be thought of as a supercooled liquid in which the viscosity is too large to permit particle rearrangement towards a more ordered form. Most of its properties depend on the conditions used to prepare it.

Our intention is to construct materials which exhibit a considerable degree of short-range order. A meaningful, yet nontrivial, two-point correlation function satisfying these conditions is

$$\tilde{S}_2(r)=\phi_2^2+\phi_1\phi_2\, e^{-r/r_0}\frac{\sin(kr)}{kr}, \tag{8}$$

where $k=2\pi/a_0$. Here r_0 and a_0 are two characteristic length scales. The overall exponential damping is controlled by the correlation length r_0, determining the maximum correlations in the system. The constant a_0 determines oscillations in the term $\sin(kr)/(kr)$ which also decays with increasing r, such that a_0 can reduce the effective range of r_0.

The various structures generated from Eq. (8) are shown in Fig. 4. They are obtained by straightforward implementation of the minimization procedure described in Sec. III. At higher densities of the black phase ϕ_2, both length scales a_0 and r_0 are clearly noticeable in the distribution of the black and white phases. At lower densities, a_0 is manifested as a characteristic repulsion among different elements with diameter of order a_0. The repulsion vanishes beyond the length scale r_0. As expected, the generated structures resemble disordered fluid configurations at lower densities.

The two-point correlation function $S_2(\mathbf{r})$ used in the construction of the structures shown in Fig. 4 are calculated at each MC step using a FFT algorithm. According to Eq. (5), $S_2(r)$ is obtained by averaging $S_2(\mathbf{r})$ over all directions. In practice, only discrete values $\mathbf{r}_{i,j}=i\hat{\mathbf{x}}+j\hat{\mathbf{y}}$, $i,j=0,1,\ldots$, are available. Thus, the lengths $|\mathbf{r}_{i,j}|$ are first categorized over bins of equal widths. The centers of the bins are taken to be the average values of all of the $\mathbf{r}_{i,j}$ which fall into them. The dependence of the target and generated $S_2(r)$s as functions of the bin centers is shown in Fig. 5.

Since the configurations of interest are rotationally isotropic, it is useful to find more efficient ways of calculating the radial functions $S_2(r)$. In Ref. 9 such a time-saving method is used to calculate $S_2(r)$. The method is based on the restricted evaluation of $S_2(r)$ only along rows and columns of the underlying lattice. The method, however, must be implemented with care. Although for large rotationally isotropic systems it is perfectly satisfactory to sample S_2 only in two orthogonal directions, this time-saving method can be problematic in the inverse, (re)construction, problem when there exists appreciable short-range order. The reason is that the subsequent optimization procedure then optimizes the system only in a finite number of chosen directions, while the rest remains mostly ''unoptimized,'' leading to unwanted anisotropy. To illustrate this point, we generate several configurations with selected densities $\phi_2=0.3$, 0.4, and 0.5 using Eq. (8) as the target function, and employing the

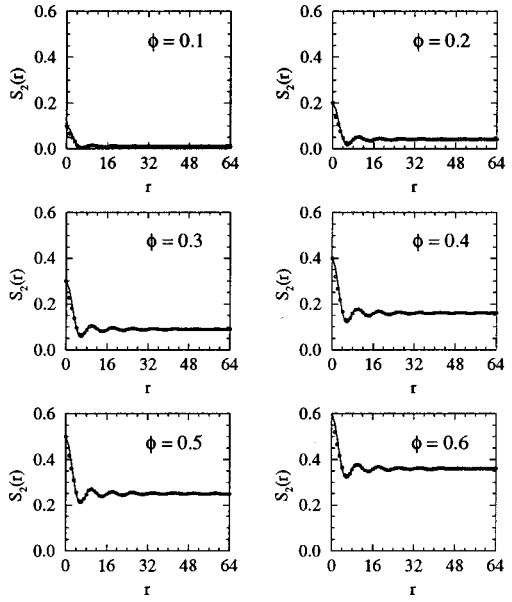

FIG. 5. Calculated (circles) and target (full lines) correlation functions $S_2(r)$ for configurations shown in Fig. 4.

sampling method of Ref. 9 with a slow cooling schedule. The results are shown in Figs. $6(a_1)$–$6(a_3)$. It is obvious that the characteristic patterns along the unoptimized diagonal directions do not reflect information contained in Eq. (8). This is more pronounced as ϕ_2 increases. Comparison of the corresponding $S_2(r)$ (calculated by sampling only in x, and y directions) with the target function [Eq. (8)] and energy evolution as a function of temperature T is shown in Fig. 7. This shows that the system can be rapidly optimized if the other possible directions are neglected which is, of course, a consequence of the oversimplification of the problem.[22] We note, however, when short-range order is absent, the time-saving orthogonal sampling method is quite accurate (see the overlapping disk and sandstone examples of Ref. 9). Moreover, the time-saving procedure also reconstructs the periodic, deterministic structures of Fig. 1 essentially perfectly.

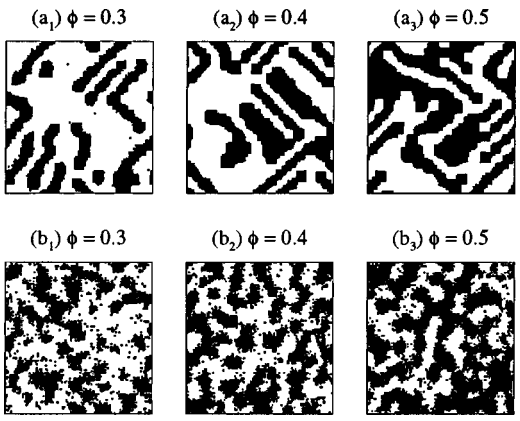

FIG. 6. Configurations for several selected densities of black phase: $\phi_2 = 0.3$, 0.4, and 0.5. They are generated by imposing conditions that their form of $S_2(r)$ mimic the one given by Eq. (8). Sampling of S_2 is performed (a) along x, and y directions only, and (b) along x, and y directions including random rotations of underlying configurations with frequency $\lambda_{rot} = 1/32$. Other parameters used in simulations are $r_0 = 32$, $a_0 = 16$, $L_x = L_y = 128$, $T_0 = 5 \times 10^{-4}$, $\lambda_{MC} = 10$, $\lambda_{tot} = 100$, and $\lambda = 0.95$.

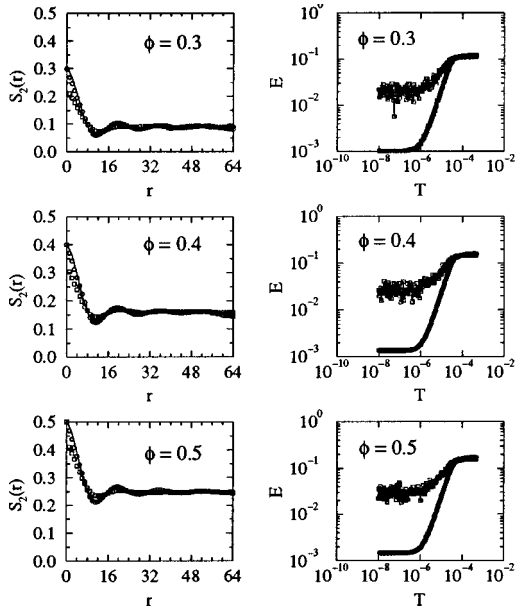

FIG. 7. Correlation functions $S_2(r)$ of target configurations given by Eq. (8) (full lines), and ones obtained from constructed configurations shown in Figs. $6(a_1)$–$6(a_3)$ (circles, or symbols closer to the full lines), and Figs. $6(b_1)$–$6(b_3)$ (squares) which are evaluated in the same way as in employed construction procedure. In E vs T plots, lower (circles) and upper (squares) curves correspond to constructions shown in Figs. $6(a_1)$–$6(a_3)$ and Figs. 6 (b_1)–$6(b_3)$, respectively.

A simple but effective way to improve the restricted-direction sampling approach is to randomize the sampling directions. This may be readily achieved, for instance, by randomly rotating underlying configurations after each $\lambda_{rot} L_x L_y$ accepted MC updates at a given T. The parameter λ_{rot} determines the frequency of the performed rotations. We notice that the rotations do not preserve the imposed periodic boundary conditions. This, however, has no relevant physical consequences since in the assumed limit $r_0 \ll L_x, L_y$, the boundaries do not affect the bulk structure. Another more important remark is related to the overall optimization procedure. Since the randomly chosen sampling directions are not simultaneously optimized, it is not likely that the algorithm will lead to a globally optimal state. Nevertheless, the procedure can efficiently find suboptimal configurations which are frequently good enough for practical purposes, as was discussed earlier.

Figures $6(b_1)$–$6(b_3)$ show several constructions of the target configurations described by Eq. (8). They were obtained using sampling in x, and y directions combined with random rotations by random angles chosen from a uniform distribution in the interval $(0, \pi/2)$. Evidently, the rotational isotropy is largely restored. On the other hand, the achieved resolution is still moderate. Figure 7 depicts the target and calculated correlation functions and energy of the systems as function of T for the two implemented methods. The biggest discrepancies are found in the small r regime. This could be significantly reduced by including, for example, the specific surface s in the objective function E. Of course, the price would be reflected in the computation time.

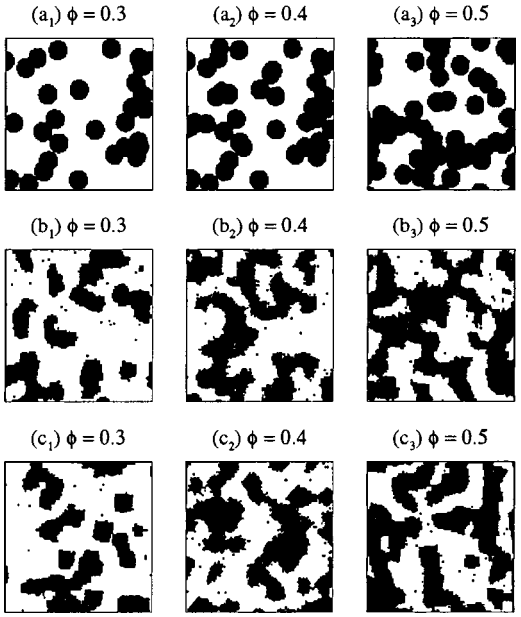

FIG. 8. Examples of (a) reference random overlapping-disk configurations, (b) S_2 reconstruction, and (c) simultaneous S_2 and L reconstruction. Parameters used in simulations are $d=16$, $L_x=L_y=128$, $T_0=5\times10^{-4}$, $\lambda_{MC}=10$, $\lambda_{tot}=100$, $\lambda=0.95$, and $\lambda_{rot}=1/8$.

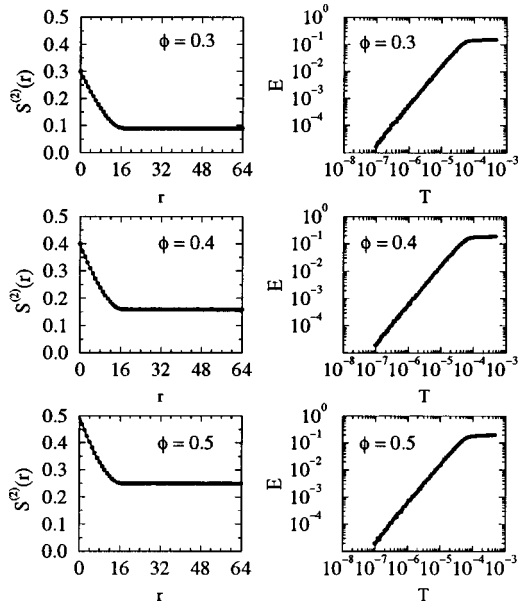

FIG. 9. Comparison of reconstructed correlation functions S_2 (circles) with reference form given by Eq. (9) (full lines). Reconstruction is performed by imposing conditions only on ϕ_2 and S_2. Corresponding energies as function of annealing temperature are also shown. Generated structures are shown in Fig. 8(b).

C. Randomly distributed overlapping disks

In this section we focus our attention on numerical reconstructions which involve several known correlation functions. As example, we choose a system of randomly distributed overlapping disks studied in Ref. 9. These systems are sometimes used in modeling configurations of real consolidated media such as porous media and sintered materials. Their main advantage is analytical tractability. Several exact results are known.[2] We will use the expression for the target two-point correlation function $\tilde{S}_2(r)$ given by[23]

$$\tilde{S}_2(r)=1-2\phi_1+\phi_1^{4f(r)/(d^2\pi)}, \tag{9}$$

with $f(r)$ given by

$$f(r)=d^2\pi/2-(d^2/2)[\arccos(r/d) -(r/d)\sqrt{1-(r/d)^2}]\Theta(d-r), \tag{10}$$

where d is the disk diameter, and Θ is the Heaviside step function. Another correlation function which we will use in the reconstruction is the lineal-path function $L(r)$ defined in Sec. II. It turns out that the easiest way to calculate this function for the particle phase is via numerical sampling over a large realization of computer-generated overlapping disks. We note that $L(r)$ for the void phase is known analytically.

In Fig. 8(a) we showed several realizations of the reference system for different volume fractions of the black phase: $\phi_2=0.3$, 0.4, and 0.5. In reconstructing these structures, we used the fast orthogonal-direction sampling procedure which involves random rotations of the underlying structure, as described above. In the first reconstruction shown in Fig. 8(b), only information on the volume fraction and the reference two-point correlation function [Eq. (9)] are used. Then we repeated the reconstruction including the constraints on the ϕ_2, $S_2(r)$, and $L(r)$ simultaneously. These results are shown in Fig. 8(c). Comparisons of the reconstructed and reference correlation functions are shown in Figs. 9 and 10.

At lower densities, there is no noticeable difference between reconstructions based on S_2 and ones which incorporate both S_2 and L. This is exactly what one would expect, since at lower densities there is no significant clustering which would be captured by L. As we increase ϕ_2 towards the percolation threshold, $\phi_2^*\approx0.68$, L is expected to make significant differences [see Figs. 8(a_3), 8(b_3), and 8(c_3)]. The

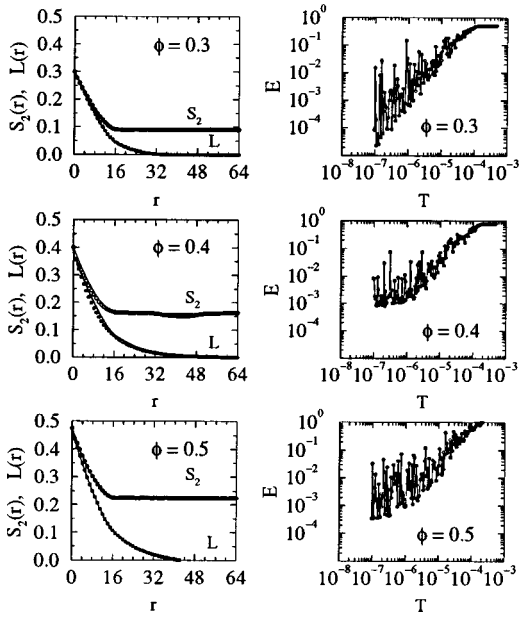

FIG. 10. Simulation details of simultaneous S_2 and L reconstruction shown in Fig. 8(c).

optimization becomes harder, which is manifested in the slower decay of the system energy as a function of T. This is evident from the comparison of Figs. 9 and 10. For larger densities the simulations should be done on larger systems for the homogeneity assumption to hold. The reason for this is that as ϕ_2^* is approached, the characteristic clustering length becomes comparable with system size.

In Sec. V, we will discuss other optimization methods and use the overlapping-disk model to study the uniqueness of the obtained solutions.

V. OTHER METHODS AND UNIQUENESS OF THE SOLUTIONS

In our analysis, we have employed the optimization procedure based on the simulated annealing technique with Metropolis acceptance rules as a global search strategy. The rules define how to move from a given configuration to another one in its neighborhood in the attempt to find the globally optimized state. After the annealing schedule is adequately chosen, the procedure works well. It has been successfully applied in all of the examples studied in this work. Here we will also test some new optimization methods (acceptance rules) which have been introduced.

According to the threshold acceptance (TA) algorithm,[24] a new configuration is accepted only if its threshold energy is less than the energy of the old one plus some predefined threshold value $E_{\text{th}}>0$, which is systematically lowered during the course of the simulation. Thus, the important difference between the simulated annealing and the TA algorithm is in the acceptance rules. While the TA procedure accepts only new configurations which are better or slightly worse than the original ones (within the limit determined by E_{th}) with a certain probability, the Metropolis rules used in the simulated annealing simulations accept in principle, every configuration but with variable probabilities. A rather simple version of the thresholding technique is the so-called ''Great Deluge'' (GD) algorithm.[25] The transition probability of the GD algorithm is given by:

$$P(E_{\text{old}}\rightarrow E_{\text{new}})=\begin{cases}1, & \text{if } E_{\text{new}}\leqslant E_{\text{th}},\\ 0, & \text{otherwise,}\end{cases} \tag{11}$$

where E_{th} is again some predefined threshold energy. After each acceptance, the value of E_{th} is usually reduced by a certain percentage of the difference between energies of the newly accepted configuration and the previous value of E_{th}. The main difference between the TA and GD algorithms is in the definition of the threshold energy E_{th}: in the GD case, E_{th} continuously decreases, whereas the TA rules allow E_{th} to increase. Also note that the GD algorithm violates the ergodicity condition since the transitions to states lying above E_{th} are not allowed. This, however, is inconsequential in our applications.

We tested the GD algorithm using it as an optimization method in the (re)construction problems described in Sec. IV, and compared the obtained results with those found by simulated annealing. Although no new physics was found, the GD algorithm has impressive performance. It gives excellent agreement between the target and generated correlation functions. It is simpler to implement, and considerably faster (an order of magnitude) than the simulated annealing technique. The significant reduction in computation time is likely related to the relatively simple energy landscape of our current optimization problems. In such cases, it is not necessary to use robust optimization algorithms such as simulated annealing which, in addition, usually must be accompanied by a rather conservative choice of the annealing schedule and this longer computational time. We note that the SA computation time for the examples studied in this article can be significantly reduced by fine tuning the annealing schedule. The choice of the best simulation parameters is important if one is interested in the comparison of the performance of different optimization algorithms. This, however, is not the purpose of this article.

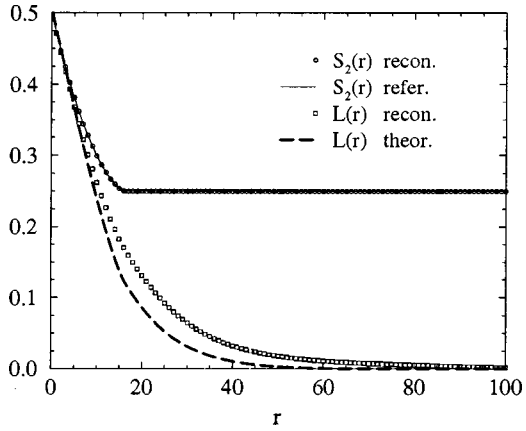

FIG. 11. Reconstruction of random overlapping disk system ($\phi_1=\phi_2=0.5$, $d=16$, $L_x=L_y=400$) using only S_2 function, and GD optimization algorithm. Lineal-path function $L(r)$ is then calculated from the reconstructed configuration and compared with the theoretically expected form.

We now turn our attention to the question of the uniqueness of the reconstructed solutions, i.e., are the higher-order correlation functions uniquely determined (statistically) by only on a few lower-order correlation functions if the global minimum is truly achieved? Of course, the character of the energy landscape determines how closely one can approach the true global minimum numerically. In general, lower-order correlation functions do not contain complete morphological information and thus they cannot uniquely characterize the microstructure, even if the global minimum is achieved. To probe the nonuniqueness question, we generated a large reference system, $L_x=L_y=400$, of randomly distributed overlapping disks with diameter $d=16$ at a volume fraction $\phi_1=\phi_2=0.5$. We then reconstructed the system employing the GD algorithm and imposed constraints only on the isotropic function $S_2(r)$. Finally, the lineal-path functions $L(r)$ were computed for both the original and the reconstructed structure. These results are shown in Fig. 11. The discrepancy between the reference (broken line) and reconstructed (squares) $L(r)$ is clearly noticeable. As an additional test, we repeated the reconstruction keeping the same constraints but using a different sequence of random numbers. Then we computed $L(r)$ again, and compared it with the one obtained from the first reconstruction. The obtained curves do not match one another. This supports the expecta-

tion that the generated microstructures do not necessarily contain the same statistical information beyond what is imposed, even though a naked-eye comparison is many times more insensitive to such differences.

Although the use of lower-order correlation functions in reconstructions cannot exactly reproduce the higher-order correlation functions of the system, such lower-order information nonetheless imposes strong constraints on the allowable microstructures. Thus, in some cases, the three- and four-point functions (which contain two-point information) of the reconstructed system may approximate well the same functions of the reference system.

VI. CONCLUSIONS

We have analyzed in detail the recently introduced stochastic optimization (re)construction method based on certain incomplete microstructural information about the system of interest. The specified information is usually given in the form of various statistical correlation functions of any type or number. The method provides a powerful tool to visualize consequences of the applied conditions. It can be used both as a method of data analysis or as a structural modeling tool to make predictions about the system. We have considered several examples, including random and deterministic systems, which are common in theoretical studies of composite materials. The (re)construction procedures were performed by employing stochastic optimization techniques, in particular, the simulated annealing method as well as some novel, ready to implement methods. We focused our attention on the kinetics of the simulation process and on the simulation details which could be of major importance to practitioners. The reliability of the solutions was investigated as well.

We found that the method can generate reliable configurations that match the imposed structural properties of random systems. One must be careful in implementing the time-saving orthogonal sampling method used in Ref. 9 when the standard two-point correlation function S_2 is utilized for systems with appreciable short-range order. In such instances, one can use Fourier transform techniques to sample in all directions but one must pay additional computational cost. Moreover, since it has been shown that S_2 is typically insufficient to accurately reconstruct a microstructure, one must be able to incorporate other correlation functions of the system which cannot be sampled using Fourier analysis. Thus, the development of time-saving sampling methods is crucial to get accurate reconstructions for general microstructures. In this article, we took a first step in this direction by suggesting an improvement of the orthogonal sampling procedure without significantly increasing computational time.

Although consistent with the conditions built in the optimization objective function or ''energy,'' the reconstructed solutions are not unique in a statistical sense. The microstructural information beyond the imposed information remains uncertain. This was demonstrated using a system of randomly distributed overlapping disks, where we showed that the computed lineal-path functions of the reconstructed systems do not match those of the original systems.

Another practical issue concerns the relation between invested computational time and the degree of achieved topological uniqueness. Based on the examples studied in Sec. IV, we found that the simulations are relatively very fast if the radial two-point correlation function is the only imposed constraint. Even simple optimization techniques (e.g., GD algorithm) are in most cases extremely efficient. However, convergence towards a globally optimal solution becomes significantly slower when more reference functions are simultaneously involved. The ''energy landscape'' becomes much rougher. In such cases, it is expected that more sophisticated optimization techniques will need to be employed. However, the general stochastic optimization technique described here will become increasingly more feasible if the trend in the increase of the speed of computers continues.

ACKNOWLEDGMENTS

The authors thank C. L. Y. Yeong for helpful discussions and A. P. Roberts for discussion concerning the Gaussian reconstruction procedure. This work was supported by the U.S. Department of Energy, OBES, under Grant No. DE-FG02-92ER14275.

[1] G. W. Milton, Phys. Rev. Lett. **46**, 542 (1981).
[2] S. Torquato, Appl. Mech. Rev. **4**, 37 (1991).
[3] G. R. Milton and M. Phan-Thien, Proc. R. Soc. London, Ser. A **380**, 305 (1982).
[4] K. A. Synder, E. J. Garboczi, and A. R. Day, J. Appl. Phys. **72**, 5948 (1992).
[5] S. Torquato, Phys. Rev. Lett. **79**, 681 (1997).
[6] A. E. Scheidegger, *Physics of Flow Through Porous Media* (Macmillan, New York, 1960).
[7] J. Rubinstein and S. Torquato, J. Fluid Mech. **206**, 25 (1989).
[8] N. Martys and E. J. Garboczi, Phys. Rev. B **46**, 6080 (1992).
[9] C. L. Y. Yeong and S. Torquato, Phys. Rev. E **57**, 495 (1998); **58**, 224 (1998).
[10] G. K. Batchelor, *The Theory of Homogeneous Turbulence* (Cambridge University Press, New York, 1982).
[11] S. D. Rice, Bell Syst. Tech. J. **23**, 282 (1944); **24**, 46 (1945).
[12] R. J. Adler, *The Geometry of Random Fields* (Wiley, New York, 1981).
[13] J. A. Quiblier, J. Colloid Interface Sci. **98**, 84 (1984), and references therein; N. F. Berk, Phys. Rev. Lett. **58**, 2718 (1987); P. M. Adler, C. G. Jacquin, and J. A. Quiblier, Int. J. Multiphase Flow **16**, 691 (1990); M. Teubner, Europhys. Lett. **14**, 403 (1991); J. Yao *et al.*, J. Colloid Interface Sci. **156**, 478 (1993); D. P. Bentz and N. S. Martys, Transp. Porous Media **17**, 221 (1994); A. P. Roberts and M. A. Knackstedt, Phys. Rev. E **54**, 2313 (1996); P. Levitz, Adv. Colloid Interface Sci. **76–77**, 71 (1998).
[14] N. G. van Kampen, J. Stat. Phys. **24**, 175 (1981).
[15] M. D. Rintoul and S. Torquato, J. Colloid Interface Sci. **186**, 467 (1997).
[16] P. Debye, H. R. Anderson, and Brumberger, J. Appl. Phys. **28**, 679 (1957).
[17] The ''energy'' E is related to the quantity commonly used in statistics as a formal goodness of fit test.
[18] S. Kirkpatrick, C. D. Gelatt, and M. P. Vecchi, Science **220**, 671 (1983).
[19] High-resolution configurations may be obtained implementing more efficient techniques developed in image analysis [see, for example, G. Winkler, *Image Analysis, Random Fields and Dynamic Monte Carlo Methods* (Springer, Berlin, 1995)], however, these techniques do not impose the original constraints on the form of the correlation functions. Rather, they are concerned with smoothing and filtering effects.
[20] W. T. Perrins, D. R. McKenzie, and R. C. McPhedran, Proc. R. Soc. London, Ser. A **369**, 207 (1779).
[21] J. P. Hansen and I. R. McDonald, *Theory of Simple Liquids* (Academic, London, 1976).
[22] In the first paper of Ref. 9, the authors constructed a system with a two-point function of the form $S_2(r) = \phi_2^2 + \phi_1\phi_2 \exp(-r/r_0)\cos(kr)$ to incor-

porate short-range order. Essentially, the time-saving orthogonal sampling method matched this S_2 exactly with $\phi_2=0.5$ and $k/r_0=8$. However, we attempted to construct the same specific case by sampling in all directions and could not match it entirely, leading us to find that it violates some nontrivial mathematical properties that physically realizable $S_2's$ must possess (although other values of ϕ_2 and k/r_0 may be allowed). Indeed, in a future paper, we will reveal some new conditions that physically realizable S_2 must obey. This example shows the utility of a successful reconstruction/construction technique.

[23] Equation (17) in the first paper of Ref. 9 should read as Eq. (9).
[24] G. Dueck and T. Scheuer, J. Comput. Phys. **90**, 161 (1990).
[25] G. Dueck, J. Comput. Phys. **104**, 86 (1993).